Physica B 535 (2018) 310–313

Contents lists available at ScienceDirect

Physica B

journal homepage: www.elsevier.com/locate/physb

Low temperature photoluminescence study of Ce^{3+} and Eu^{2+} ions doped SrF_2 nanocrystals

Mubarak Y.A. Yagoub[a,b,*], Hendrik C. Swart[a], R.E. Kroon[a], Elizabeth Coetsee[a,**]

[a] Department of Physics, University of the Free State, PO Box 339, Bloemfontein ZA9300, South Africa
[b] Department of Physics, Sudan University of Science and Technology, Khartoum, Sudan

ARTICLE INFO

Keywords:
Photoluminescence
Lifetime
SrF_2:Eu^{2+}
SrF_2:Ce^{3+}

ABSTRACT

The photoluminescence properties of Eu^{2+} and Ce^{3+} doped SrF_2 have been reported at room temperature and 77 K. The emission spectra of Eu^{2+} ions in SrF_2 consisted of a broad band assigned to the 5d-4f transition of the Eu^{2+} ion. Ce^{3+} ions in SrF_2 showed a weak emission intensity. The emission intensity of Eu^{2+} ion was greatly enhanced at 77 K. At room temperature and 77 K, the fluorescence decay of Eu^{2+} and Ce^{3+} ions in SrF_2 have been measured and the fluorescence decay curve have been reported.

1. Introduction

Fluoride nanocrystals such as MF_2 (M=Ca, Sr, Ba) doped with lanthanide ions are widely used as phosphor materials because of their stability, non-hygroscopic and transparency behavior [1]. The structure of these materials consists of a simple cubic array of F^- ions with every alternate cube occupied by the divalent cation, M^{2+} ion. This makes the MF_2 compound efficient phosphor over a wide range of lanthanide ion concentrations. The trivalent lanthanide (Ln^{3+}) ions substitute M^{2+} and may reside in a variety of sites. The extra charge of Ln^{3+} ions is compensated by F^- anion charges, situated elsewhere in an interstitial site and form a cubic symmetry (O_h) with tetragonal (C_{4v}) or trigonal (C_{3v}) centers [2,3]. These phosphors have been regarded as excellent phosphors due to their highly efficient luminescence centers contributed by activators, Ce^{3+} and Eu^{2+} ions, which are used as scintillators [4].

The spectra and position of the 5d-4f emission bands of Ce^{3+} and Eu^{2+} ions depend on the crystal field of the host which splits the 5d level. With increasing crystal field strength the 5d states become lower in energy than the 4f states and it gives luminescence from 5d-4f transition. This shifts the luminescence from Ce^{3+} and Eu^{2+} ion to longer wavelength. Such transitions involve the vibration modes and emission exhibiting a Stoke's shift [5]. MF_2 doped with Eu^{2+} ions have been intensively studied in recent years due to their high efficiency [6–8]. Since the absorption of the 4f-5d transitions of the doping ions extends to the visible, they are appropriate phosphors for excitation by near-UV for various applications [7,8]. The Eu^{2+} emission consists of a broad band corresponding to the transition from the lower $4f^65d^1$ state to the $4f^7$ ground state. Because the position of Eu^{2+} emission is strongly dependent on the Eu^{2+} environment, the energy of the emission is determined by the choice of the M^{2+} elements. For example, Eu^{2+} doped SrF_2 emits blue light centred at 420 nm [9]. The luminescent properties of Ce^{3+} doped MF_2 have been extensively studied by several workers [2,3,10]. The absorption spectrum consists of two bands, which are attributed to the 4f → 5d absorption of Ce^{3+} ions' charge compensated by F^- interstitials in the nearest-neighbor positions that form tetragonal centers. Excitation within the absorption bands reveals the characteristic emission of the Ce^{3+} ions in tetragonal sites, which consists of two bands peaking at 320 and 340 nm. These bands are associated with transitions from the $^2D_{3/2}$ excited level to the $^2F_{5/2}$ and $^2F_{7/2}$ ground state components by spin–orbit interaction [2,3]. Eu^{2+} and Ce^{3+} doped SrF_2 are promising phosphors for down-conversion applications in solar cells. They act as sensitizers to feed the low absorption transitions of Ln^{3+} ions. The energy transfer from Eu^{2+} and Ce^{3+} to the Ln^{3+} ions has been expected to be highly efficient [10]. This is due to the low phonon energy and extended transparency of the SrF_2 host, resulting in high spontaneous emission probabilities, large emission cross-sections and low non-radiative decay rates between energy levels of the doped ions. SrF_2 doped with Pr^{3+} and Yb^{3+} couple exhibits excellent quantum cutting but the weak absorption cross-section of the 4f-4f transition of the Pr^{3+} ion is, however, an obstacle to investigate such a promising efficiency enhancement. One suggestion worthwhile to investigate, is to add a third sensitizer [11]. The excellent quantum efficiency from Pr^{3+} and Yb^{3+} ions in the SrF_2 host is due to the low phonon energy of the host which is about 350 cm^{-1} compared to CaF_2 which is about 495 cm^{-1} [12,13]. In this work, we studied the luminescence of SrF_2:Eu^{2+} and SrF_2:Ce^{3+} phosphors at 77 K and room

* Corresponding author at: Department of Physics, University of the Free State, PO Box 339, Bloemfontein ZA9300, South Africa.
** Corresponding author.
E-mail addresses: mubarakyagoub@sust.ac.za (M.Y.A. Yagoub), coetseee@ufs.ac.za (E. Coetsee).

http://dx.doi.org/10.1016/j.physb.2017.08.011
Received 18 April 2017; Received in revised form 1 August 2017; Accepted 3 August 2017
Available online 04 August 2017
0921-4526/

temperature. Data was obtained at low temperatures in order to study the effect of the temperature on the wide emission and the position of Ce^{3+} and Eu^{2+} ions in fluoride materials. The results serve as pre-investigation to study the down-conversion mechanism from Eu^{2+} and Ce^{3+} to Ln^{3+} ions at low temperature for solar cell applications.

2. Experimental

Eu^{2+} and Ce^{3+} doped and undoped SrF_2 phosphor samples were synthesized by the hydrothermal method. For the hydrothermal process, all chemical reagents were of analytical grade and were used without further purification. For a typical synthesis, 1 mmol of $Sr(NO_3)_2$ was first dissolved in 30 mL distilled water, followed by 5 mmol of $Na_2C_{10}H_{14}N_2O_8{\cdot}2H2O$ (Na_2EDTA, ethylenediamine tetra-acetic acid disodium salt) and 2 mmol of $NaBF_4$ under constant stirring. After further magnetic stirring for 10 min the solution was transferred into a 125 mL autoclave lined with Teflon, heated at 160 °C for one hour and naturally cooled down to room temperature [19]. The product was collected by centrifugal and washed with water and ethanol. Finally, the product was dried for 10 h in an oven at 60 °C. Eu^{2+} doped SrF_2 samples were prepared by the same hydrothermal technique, $Eu(NO_3)_3(H_2O)_5$ and $Ce(NO_3)_3(H_2O)_6$ were used as sources for the Eu^{2+} and Ce^{3+} dopants, respectively. The SrF_2: Eu^{2+} sample was annealed under a reducing atmosphere (Ar 95%/H_2 5%) for 2 h in order to reduce Eu^{3+} into Eu^{2+} ions.

The structure of the prepared samples was characterized by X-ray diffraction (XRD) using a Bruker Advance D8 diffractometer (40 kV, 40 mA) with Cu K_α x-rays (λ = 0.154 nm). The photoluminescence spectra at low and room temperature were collected with Edinburg instrument FS980. All lifetimes were measured with nF20 nanosecond flashlamp. All the measurements at 77 K were performed using a liquid nitrogen cryostat.

3. Results and discussion

The XRD patterns of the undoped and Ce^{3+} and Eu^{2+} doped SrF_2 powder as well as the standard data for SrF_2 (card No. 00-086-2418) are shown in Fig. 1. The doped samples crystallized into the face centred cubic phase with the *Fm3m* space group and a lattice parameter of 5.785 ± 0.005 Å. It can also be seen that all observed peaks match well with the reference data, which indicates that there was no obvious influence of the dopants on the crystalline structure of the host. Doping with Ce^{3+} and Eu^{2+} resulted in a small shift to higher Bragg's angles (9.0% and 14% for Ce^{3+} and Eu^{2+}, respectively) with comparison to the un-doped sample and the standard data. This is

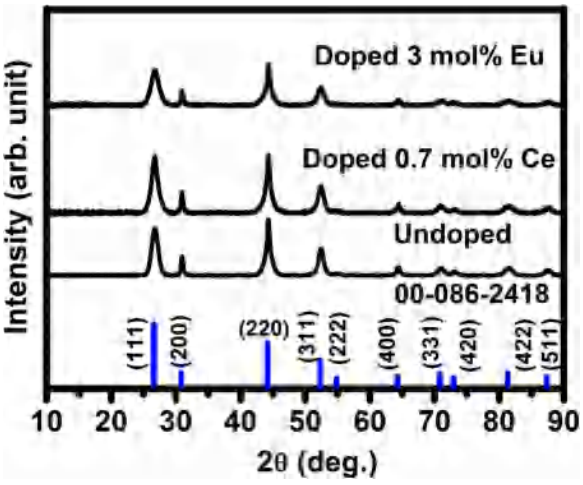

Fig. 1. X-ray diffraction patterns of un-doped SrF_2, SrF_2:Ce^{3+} and SrF_2:Eu^{2+} samples. The standard data of the SrF_2 crystal from card number ICSD 00-086-2418.

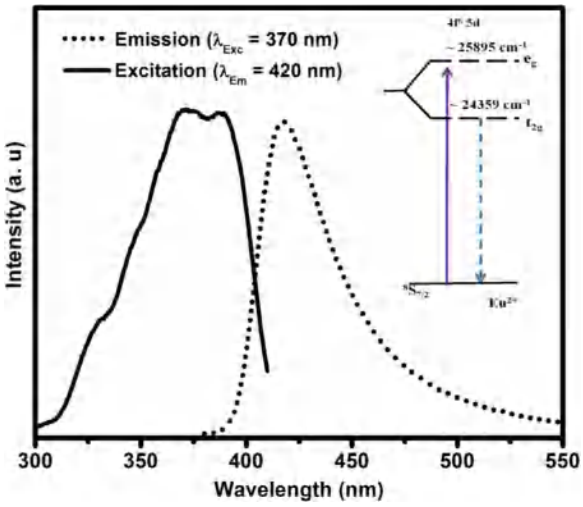

Fig. 2. Excitation spectrum (solid line) and emission spectrum (dotted line) of SrF_2:Eu^{2+} (3 mol%) at room temperature. The inset graph is a schematic energy level diagram of the Eu^{2+} doped SrF_2 [14].

attributed to the radius difference between Eu^{2+} (0.125 nm), Eu^{3+} (0.107 nm), Ce^{3+} (0.114 nm) and Sr^{2+} (0.126 nm) [6], which confirms that Ce^{3+} and Eu^{2+} ions were successfully incorporated into the SrF_2 lattice.

Fig. 2 represents the relationship between the excitation and emission spectra of SrF_2:Eu^{2+} (3 mol%) at room temperature. The spectra clearly consist of broad excitation and emission bands. The excitation spectrum consists of two main bands with maxima at 370 and 387 nm. The 5d states of Eu^{2+} are split into two sets of the energy levels, which can be designated by t_{2g} (the lowest) and e_g (the highest), see inset graph in Fig. 2. The O_h group notation is used here for these levels, although actual crystal field of low symmetry will split these levels further. The energy separation between the t_{2g} and e_g states is called the crystal field strength. The Eu^{2+} luminescence is usually observed only from the lowest $4f^65d^1$ state since the higher excited states are easily relaxed to the lowest $4f^65d^1$ state located below the bottom of the conduction band. The result showed that the phosphor exhibits a blue emission peaked at 420 nm. This broad band is attributed to the inter-configuration $4f^65d^1$-$4f^7$ allowed transition of the Eu^{2+} ion [6,10]. No emission peaks of Eu^{3+} were observed in the emission spectra indicating that the Eu^{3+} ions in the sample have been completely reduced to Eu^{2+} ions.

Fig. 3(a) portrays a comparison between the photoluminescence excitation spectra of the SrF_2:Eu^{2+} (3 mol%) at 77 K and room temperatures. The excitation spectra at both 77 K and room temperature were obtained by monitoring the emission of Eu^{2+} centred at 420 nm. The broad excitation spectrum (blue curve) that measured at 77 K temperature related to Eu^{2+}:$4f^7$–$4f^65d$ transition consists of several small peaks. This is related to the crystal field splitting of the Eu^{2+} energy levels as discussed earlier. The levels of the actual crystal field of low symmetry will split further. It is well known that the $4f^65d$ state of Eu^{2+} is very sensitive to changes in crystal field strength, which leads to the splitting of the main levels into sublevels depending on strength [15]. This might be the reason that the excitation band measured at 77 K split into sublevels as clearly seen in Fig. 3(a).

The emission transition is expected to occur only from the lowest 5d level, according to the general shape of the photoluminescence band. The emission spectra at room temperature and 77 K are presented in Fig. 3(b). In this study only one band was observed at room temperature and liquid nitrogen. However, luminescence from a higher Eu^{2+} $4f^65d^1$ state may be observed due to the absence of high energy lattice vibrations at low temperature. Luminescence from a higher Eu^{2+} $4f^65d^1$ state has been reported in different hosts [16]. However, with increasing temperature, the electron–phonon interaction in both the

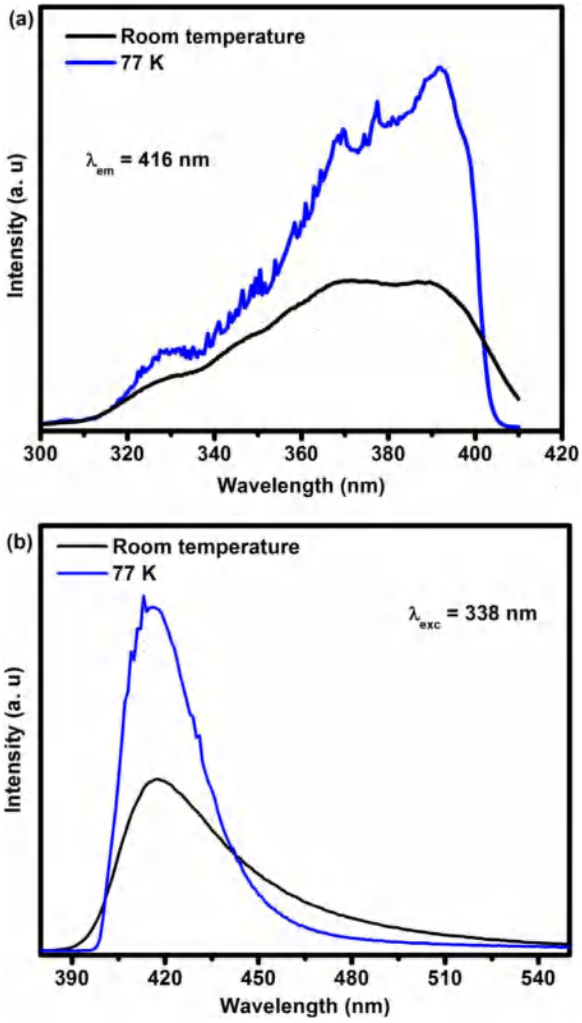

Fig. 3. Comparison between 77 K and room temperature (a) excitation spectra and (b) emission spectra of SrF_2:Eu^{2+} (3 mol%).

ground state and excited states of the luminescence center becomes dominant resulting in broadening of the emission spectra and decrease of the emission intensity [17]. In this study, the width (FWHM) of the room temperature emission band values 42 nm and 28 nm for 77 K. This can be attributed to the absence of high energy lattice vibrations at low temperature. Furthermore, the luminescence intensity decreased at the room temperature measurement. The effect of decreasing integrated PL intensity in real experiments can be explained by thermal quenching. It means that at high temperature both non-radiative and radiative transitions are present, while at low temperature the non-radiative transitions are negligible.

The emission spectra of the SrF_2:Ce^{3+} (0.7 mol%) for (a) 77 K and (b) room temperature are shown in Fig. 4. The emission was collected by exciting the crystal within 295 nm. The emission spectrum consists of two bands, peaking at 307 and 328 nm. These emission bands correspond to the parity allowed transition of the lowest component of the excited state $^2D_{3/2}$ to the split ground state into their $^2F_{5/2}$ and $^2F_{7/2}$ components, see inset graph in Fig. 4, which agreed well with previous studies [2,18]. The intensity ratio between these two components decreased at 77 K (Fig. 4(a)). This might be due to the low phonon energy at low temperature which limits the energy transfer between these two components.

The decay curves of the Eu^{2+} emission in SrF_2 were measured at 77 K and room temperature (Fig. 5(a)). The decay curve at 77 K could be fitted with a single exponential. Whereas, the decay curve at room temperature could only be fitted with a second order exponential decay

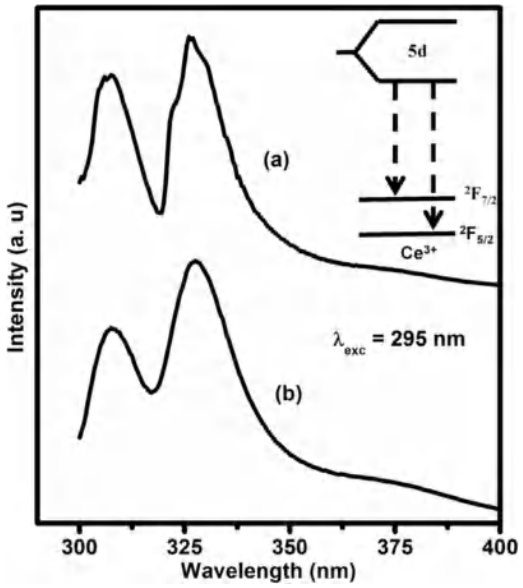

Fig. 4. Emission spectra of Ce^{3+} (0.7 mol%) at (a) 77 K and (b) room temperature. The inset graph is the energy level diagram of Ce^{3+} [14].

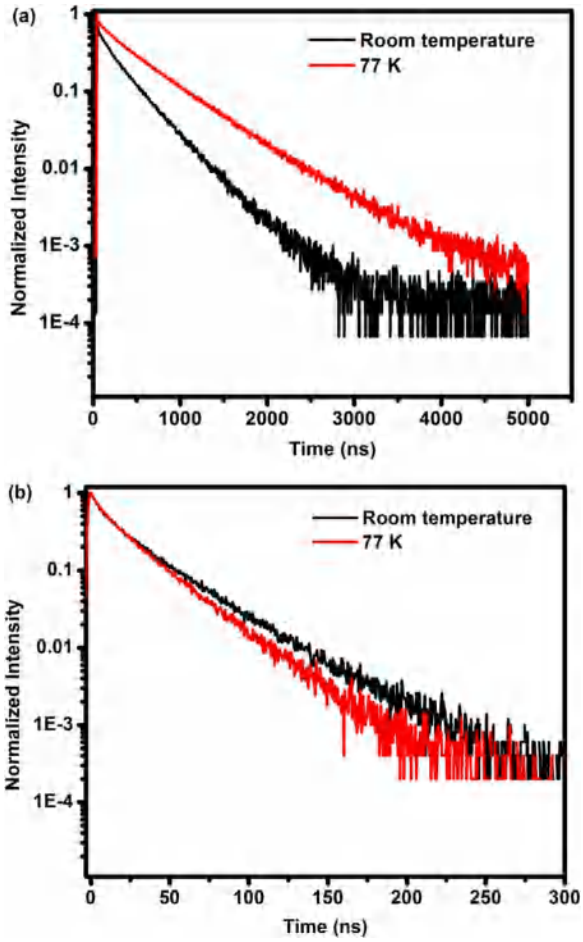

Fig. 5. Decay curves at room temperature and 77 K of (a) Eu^{2+} 5d (monitoring 420 nm emission) under 370 nm excitation (b) Ce^{3+} 5d (monitoring 328 nm emission) under 295 nm excitation.

mode with decay model $I(t) = A_1 \exp(-t/\tau_1) + A_2 \exp(-t/\tau_2)$, demonstrating the interaction between Eu^{2+} ions that takes place at room temperature. The average decay time τ can be determined by the formula given in the following equation: $\tau = (A_1 \tau_1^2 + A_2 \tau_2^2)/(A_1 \tau_1 +$

A_2 τ_2). A_1 and A_2 are constants, and τ_1 and τ_2 are the short- and long-decay components, respectively. At room temperature, the levels are populated, therefore a strong decrease of the decay time of SrF_2:Eu^{2+} is observed. The decreased decay times can be attributed to increase interaction between Eu^{2+} ions when rising the temperature.

The decay curves of the Ce^{3+} emission in SrF_2 were measured at 77 K and room temperature (Fig. 5(b)). Due to the closeness of the excitation and lower wavelength Ce emission peak, we measured the lifetime to the longer emission peak at 328 nm. Strangely this lifetime got shorter when cooled. This situation is not fully understood and is still under investigation. The 4f-5d transition of Eu^{2+} and Ce^{3+} is a fully allowed transition. This makes these ions absorb most of the incident energy. The light yield in case of room temperature is, however, less due to the absence of high energy lattice vibrations at low temperature. It means that the temperature dependence is essential and must be taken into account.

4. Conclusion

The studied materials were successfully synthesized by hydrothermal technique. The structure of the material was characterized by XRD and found to be single phase. The photoluminescence properties of Eu^{2+} and Ce^{3+} doped SrF_2 was studied at room temperature and 77 K. The emission spectra of Eu^{2+} ion in SrF_2 consist of a broad band assigning to the 5d-4f transition of Eu^{2+} ion. The FWHM of the room temperature emission band value was found to be 42 nm and 28 nm for 77 K. Ce^{3+} ion in SrF_2 shows very weak emission intensity compared to SrF_2:Eu^{2+} emission. The decay lifetime of Eu^{2+} was observed to decrease at room temperature. The decreased decay times can be attributed to increase interaction between Eu^{2+} when rising temperature.

Acknowledgments

This work is based on the research supported by the South African Research Chairs Initiative of the Department of Science and Technology and National Research Foundation of South Africa (84415) and the National Research Foundation NEP program of South Africa (93214). The financial assistance of the National Research Foundation (NRF) and the University of the Free State towards this research is hereby acknowledged.

References

[1] K.V. Ivanovskikh, V.A. Pustovarov, M. Krim, B.V.J. Shulgin, Appl. Spectr. 72 (2005) 564–568.
[2] U.G. Caldino, C. de la Cruz, G.H. Munoz, J.O. Rubio, Solid State Commun. 69 (1989) 347–351.
[3] U.G. Caldino, J. Phys.: Condens. Matter 15 (2003) 3821–3830.
[4] R. Shendrik, E.A. Radzhabov, A.I. Nepomnyashchikh, Radiat. Meas. 56 (2013) 58–61.
[5] M. Nazarov, A. Nor Nazida, S.C.M. Calyn, N.M.A. Aziz, M.N. Ahmad-Fauzi, Moldavian J. Phys. Sci. 11 (2012) 67–77.
[6] M.Y.A. Yagoub, H.C. Swart, L.L. Noto, J.H. O'Connell, M.E. Lee, E. Coetsee, J. Lumin. 156 (2014) 150–156.
[7] M.E. Lee, J.H. O'Connell, M.Y.A. Yagoub, H.C. Swart, E. Coetsee, Phys. B: Condens. Matter 480 (2016) 169–173.
[8] Weihao Ye, Qiying Huang, Xiaotang Liu, Guangqi Hu, Acta Mater. 122 (2017) 420–430.
[9] M.Y.A. Yagoub, H.C. Swart, M.S. Dhlamini, E. Coetsee, Opt. Mater. 60 (2016) 521–525.
[10] M.Y.A. Yagoub, H.C. Swart, P. Bergman, E. Coetsee, AIP Adv. 6 (2016) 025204–025215.
[11] B.M. Van der Ende, L. Aarts, A. Meijerink, Phys. Chem. Chem. Phys. 11 (2009) 11081–11095.
[12] M.Y.A. Yagoub, H.C. Swart, E. Coetsee, Opt. Mater. 42 (2015) 204–209.
[13] P.A. Ballea, A.S. Uganuma, F.D. Ruon, J.H. Ostalrich, P.G. Eorces, P.G. Redin, M.M. Ortier, Optica 2 (2015) 288–291.
[14] T. Hoshina, J. Phys. Soc. Jpn. 48 (1980) 1261–1268.
[15] R.B. Jabbarov, C. Chartierb, B.G. Tagiev, O.B. Tagiev, N.N. Musayeva, C. Barthou, P. Benalloul, J. Phys. Chem. Solids 66 (2005) 1049–1056.
[16] M. Nazarov, B. Tsukerblat, D.Y. Noh, J. Phys. Chem. Solids 69 (2008) 2605–2612.
[17] Q. Wang, G. Zhu, S. Xin, X. Ding, J. Xu, Y. Wang, Y. Wang, Phys. Chem. Chem. Phys. 17 (2015) 27292–27299.
[18] M. Zahedifar, E. Sadeghi, M.R. Mozdianfard, E. Habibi, Appl. Radiat. Isot. 78 (2013) 125–131.